PHYSICAL REVIEW A VOLUME 46, NUMBER 9 1 NOVEMBER 1992

# General theory of temperature-dependent ultrafast transient hole burning

A. A. Villaeys and J. C. Vallet
*Institut de Physique et Chimie des Matériaux de Strasbourg, Groupe d'Optique Nonlinéaire et d'Optoélectronique, 5, rue de l'Université, 67084 Strasbourg-CEDEX, France*

H. Ma and S. H. Lin
*Department of Chemistry and Center for the Study of Early Events in Photosynthesis, Arizona State University, Tempe, Arizona 85287-1604*

(Received 30 March 1992)

In this paper, we report the theoretical treatment of ultrafast time-resolved hole burning. The description is valid for nonoverlapping and overlapping pulses as well. Also the effects of the temperature are included in the theory. The influence of the various contributions to the transient hole-burning spectrum corresponding to the level population, pump polarization coupling, and perturbed free-induction-decay terms is stressed.

PACS number(s): 42.65.Re, 42.65.Hw

## I. INTRODUCTION

During the past decade, a large number of coherent optical spectroscopies have been developed to probe the internal dynamics of molecules in the gas or condensed phase [1–4]. Among these techniques, such as photon echo [5], coherent Raman spectroscopy [6], photon correlation spectroscopy [7], and polarization spectroscopy [8], which have been used to study optical dynamics, hole burning has played a particular role because of its simple and straightforward application to large varieties of systems [9,10].

In most solid-state hole-burning experiments, the time delay between the pumping and probing pulses is longer than any dynamical time constant of the molecular system. Therefore, if the experiments are envisioned as a particular four-wave-mixing process, the possible interference effects due to the simultaneous presence of the pump and probe beams do not contribute. As a consequence, among all the contributions participating in the four-wave mixing, only those where two pump beam interactions generate an excited level population which is next tested by the probe beam are accounted for. This is because, for long time delay, only these terms survive. Finally, the time-varying polarization resulting from the four-wave mixing induces in the probing direction a frequency-dependent energy loss of the probe beam. It is just this variation which is known as the hole-burning effect.

In solution, most of the hole-burning experiments have been performed with pulse durations long enough to establish a steady-state regime on the system. Here, a narrow-band laser is used to burn a hole in the optical absorption spectrum of the molecules which are probed by a time-coincident broadband laser. This technique has been frequently employed. However, it did not enable determination of the time scale of the dynamical processes in solution and many conflicting results were published concerning the magnitude of their optical dephasing constants [11–14].

With the rapid development in experimental and theoretical approaches of ultrafast processes [15–19] and the ultrashort laser pulses now available, it is possible to make observations on a time scale shorter than or comparable to the molecular vibrational periods. This has enabled the recent femtosecond time-resolved hole-burning experiments on solutions which have unambiguously established the ultrafast character of the dynamical processes taking place on solutions. Here, because of the high time resolution, the validity of the experimental results is not questionable and even the apparent discrepancy between the results recently obtained from femtosecond time-resolved hole-burning [20] and photon echo experiments [21,22] has been clarified as resulting from the nature of the initially prepared state. At this point, it has to be mentioned that for very short experimental time resolution, non-Markovian effects become relevant and consequently the dephasing processes cannot any longer be described by a time constant $T_2$. As an example, from the recent femtosecond photon echo experiment done in solution by Nibbering, Wiersma, and Duppen [23], it is clear that solution dynamics cannot be described by phenomenological Bloch equations.

However, the observation of spectral holes in solution may be difficult and hole burning should be observed at very short time delay. Consequently, the pump-and-probe pulses overlap and additional processes contribute to the spectrum. Recently, Brito Cruz *et al.* [24] have introduced a four-wave-mixing description of pump-probe spectroscopy for a two-level system with hyperbolic sequant-square intensity femtosecond pump and probe pulses. They have established that the signal arising in a transient hole-burning experiment can be separated in three contributions. The first one, defined as the level population term, reflects the dynamics of the material system. It corresponds to the usual hole-burning picture, where two pump pulses create some excited-state population which is next tested by the probe pulse. The second

©1992 The American Physical Society

contribution, known as the pump polarization coupling term, follows the chronological ordering pump-probe-pump interactions. Its contribution is large if the pump and probe pulses overlap. In addition, its temporal behavior follows the pump pulse profile. The third contribution, called the perturbed free-induction-decay term, is characterized by the chronological ordering probe-pump-pump interactions. It strongly modifies the signal when the probe pulse precedes the pump pulse. It increases with time constant $T_2$. This contribution vanishes rapidly for positive delay times.

More recently, Ferwerda, Terpstra, and Wiersma [25] have shown, by using stochastic light beams with broad temporal profiles but correlation times smaller than the relaxation and dephasing constants $T_1$ and $T_2$ of the medium, that coherent artifacts with the same spectral width are detected in the probe direction $\mathbf{k}_p$, as well as in the signal direction $2\mathbf{k}_e - \mathbf{k}_p$, where $\mathbf{k}_e$ is the wave vector of the pump beam. Moreover, these artifact contributions arise from terms which have been identified with stimulated resonance Raman gain [26] and, in contrast to the previous conclusions [27] predicting peaks at the excited-state vibrational frequency, their analysis exhibits peaks at both the ground- and excited-state vibrational frequencies. Finally, a number of limitations on measuring solvent motion with ultrafast transient hole burning have been examined. Among the limitations, spectral diffusion and spectral congestion are shown to perturb the determination of the homogeneous linewidth. They conclude that transient hole burning cannot be observed in liquids. The effects of these limitations have been demonstrated experimentally for iodine in hexane [26,27].

In order to understand the dynamics as well as to disentangle the contributions associated to various mechanisms of the interactions, it is convenient to separate the spectral broadening into homogeneous components induced by very rapid interactions and inhomogeneous components resulting from slowly varying interactions. In this paper, we shall theoretically treat ultrafast transient hole burning which holds the prospect of both separating these components and directly measuring the rate of the homogeneous component. While conventional hole-burning experiments have been commonly applied to glasses and biological systems [28–33], recently, Loring, Yan, and Mukamel [34] have theoretically studied the time-resolved hole burning. However, they only treat the case of nonoverlapping laser pulses, that is, the case where pump and probe pulses do not overlap. Laubereau and his co-workers [35,36] have developed and reported the application of picosecond time-resolved hole burning to study the dynamics of inhomogeneously broadened molecular systems. In their experiments, the pump and probe pulses overlap. All these results, as well as the temperature dependence on transient hole burning, have motivated the present study.

In Sec. II, the general theory to describe transient hole burning as a particular four-wave-mixing process is presented. It enables us to introduce the third-order polarization which is required to evaluate the differential transmittance. Section III is devoted to the explicit evaluation of its frequency dependence, assuming a material system initially thermalized. While these expressions are quite general, in Sec. IV we focus on a particular four-level system which is the simplest system to account for temperature effects. Finally, in Secs. V–VII the transient hole-burning spectrum is calculated and numerical calculations have been done to emphasize the role of temperature as well as dephasing processes.

## II. GENERAL DESCRIPTION AND FORMALISM

In a transient hole-burning experiment, the molecular system is subjected to two time-delayed light pulses. The pump pulse, with wave vector $\mathbf{k}_e$ and central frequency $\omega_e$, produced by a narrow-band dye laser is used to selectively pump an optically resonant medium. Because of the local changes of the environment, the electronic transition frequency of the molecules in condensed phase has a static distribution which generates an inhomogeneous broadening of the linear absorption line shape. After some period of time, corresponding to the time delay of the light pulses, the probe pulse emitted by a broadband dye laser tests the population previously created in the sample. The physical observable of interest is the transient hole-burning spectrum. It corresponds to the variation of the probe beam intensity as a function of the frequency. For weak light beams, the differential transmittance, defined as the imaginary part of the susceptibility without the pump pulse minus the susceptibility with the pump pulse, takes the form [37]

$$\Delta\alpha(\omega) \propto \omega\,\mathrm{Im}[P^{(3)}_{\mathbf{k}_p}(\omega)/E_p(\omega)] \ , \tag{2.1}$$

which is the lowest-order term in the pump and the probe light beams. Here, $\mathbf{E}_p(\omega)$ is the Fourier transform of the $\mathbf{k}_p$ component of the probe electric field while $\mathbf{P}^{(3)}_{\mathbf{k}_p}(\omega)$ is the Fourier transform of the third-order component of the polarization in the $\mathbf{k}_p$ direction. Finally, the symbol Im stands for the imaginary part of the expression.

The theoretical framework required to evaluate the differential transmittance given by relation (2.1) is introduced in this section. It will enable us to calculate the dynamical evolution of the medium coupled to the pulsed pump and probe light beams.

The evolution of the total system is derived from the Liouville equation

$$\frac{\partial\rho(t)}{\partial t} = -\frac{i}{\hbar}[L_0 + L_V(t)]\rho(t) - \Gamma\rho(t) \ , \tag{2.2}$$

where $L_V(t)$ represents the Liouville operator for the interaction $V(t)$ between the molecules and the radiation fields. The operator $V(t)$ consists of the contributions from the pumping field $V_e(t)$ and probing field $V_p(t)$. Therefore we have

$$V(t) = V_e(t) + V_p(t) \ . \tag{2.3}$$

In the dipole approximation, they take the forms

$$V_j(t) = -\boldsymbol{\mu}\cdot[\mathbf{E}_j(\omega_j)e^{-i\omega_j t} + \mathbf{E}_j^*(\omega_j)e^{i\omega_j t}]L_j(t) \ , \quad j = e,p \ , \tag{2.4}$$

where $L_e(t)$ and $L_p(t)$ denote the laser pulse shape functions. For the sake of convenience, we shall choose

$$L_j(t)=e^{-\gamma_j|t_j-t|}\ , \tag{2.5}$$

where $t_e$ and $t_p$ represent the pumping and probing times, respectively, $T_e=\gamma_e^{-1}$ and $T_p=\gamma_p^{-1}$ denote the corresponding pumping and probing pulse durations, and $H(t)$ stands for the Heaviside function. Finally, $\Gamma$ represents the usual damping operator and $L_0$ the molecular Liouvillian.

To solve Eq. (2.2), we set

$$\rho(t)=\exp\left[-\frac{i}{\hbar}L_0' t\right]\sigma(t)\ , \tag{2.6}$$

where the notation

$$L_0'=L_0-i\hbar\Gamma \tag{2.7}$$

has been introduced. The formal solution can be expressed as

$$\sigma(t)=\sigma(t_0)-\frac{i}{\hbar}\int_{t_0}^{t}d\tau\, e^{(i/\hbar)L_0'\tau}L_V(\tau)e^{-(i/\hbar)L_0'\tau}\sigma(\tau)\ , \tag{2.8}$$

and is in a convenient form to get an iterative solution. Using the perturbation expansion, we find

$$\rho^{(n)}(t)=-\frac{i}{\hbar}\int_{t_0}^{t}d\tau\, e^{-(i/\hbar)L_0'(t-\tau)}L_V(\tau)\rho^{(n-1)}(\tau) \tag{2.9}$$

for $n>1$. Here, $\rho^{(n)}(t)$ represents the $n$th-order contribution to the density matrix. To treat transient hole burning, the third-order term $\rho^{(3)}(t)$ is needed to calculate the third-order polarization

$$\mathbf{P}^{(3)}(t)=\mathrm{Tr}[\rho^{(3)}(t)\boldsymbol{\mu}]\ . \tag{2.10}$$

This is the basic quantity which is required to get any information on the system. In the following, we will not introduce the rotating-wave approximation. This is because, in the perturbation approach, all the terms can be obtained on the same footing. However, as will be shown in the next sections, this assumption can be introduced quite easily, if required.

Finally, in order to calculate the hole-burning spectra, we still require the Fourier transform of the fields and of the polarization. With respect to the probe light beam, we have

$$\mathbf{E}_p(\omega)=\int_{-\infty}^{+\infty}dt\ \mathbf{E}_p(t)e^{i\omega t}\ . \tag{2.11}$$

With the simplifying notation

$$\mathbf{E}_j(t)=\sum_{\epsilon_j=\pm 1}\mathbf{E}_j(\epsilon_j)e^{-it\omega_j\epsilon_j}L_j(t)\ , \tag{2.12}$$

where

$$\mathbf{E}_j(1)=\mathbf{E}_j(\omega_j),\quad \mathbf{E}_j(-1)=\mathbf{E}_j^*(\omega_j)\ , \tag{2.13}$$

we get the expression

$$\mathbf{E}_p(\omega)=\sum_{\epsilon_p=\pm 1}\mathbf{E}_p(\epsilon_p)e^{i(\omega-\omega_p\epsilon_p)\bar{t}_p}\frac{2\gamma_p}{(\omega-\omega_p\epsilon_p)^2+\gamma_p^2}\ . \tag{2.14}$$

It has to be noted that, according to the phase-matching conditions, we will have to select only one component of the probe beam. This will be done by taking the convenient value of $\epsilon_p$. It can also be mentioned here that, because of the particular geometry used in a hole-burning experiment, the contributions satisfying the phase-matching conditions are exactly those which participate in the $\mathbf{k}_p$ component of the polarization. To conclude this section, we still have to introduce from expressions (2.9) and (2.10) the polarization

$$\mathbf{P}^{(3)}(t)=-\frac{i}{\hbar}\int_{-\infty}^{t}d\tau\,\mathrm{Tr}[e^{-(i/\hbar)L_0'(t-\tau)}L_V(\tau)\rho^{(2)}(\tau)\boldsymbol{\mu}]\ , \tag{2.15}$$

which can be expressed as a convolution product. Therefore its Fourier transform is given by the expression

$$\mathbf{P}^{(3)}(\omega)=-\frac{i}{\hbar}\mathrm{Tr}[\mathcal{F}(e^{-(i/\hbar)L_0't})\mathcal{F}(L_V(t)\rho^{(2)}(t))\boldsymbol{\mu}]\ . \tag{2.16}$$

It will be evaluated in the following sections to study the transient hole-burning spectrum observed in some molecular compounds.

## III. EVALUATION OF THE FREQUENCY-DEPENDENT POLARIZATION

In order to extract physical informations from transient hole-burning spectra, we must focus on some particular system. For the problem at hand, we can restrict the dynamics of the system to two electronic configurations in the presence of one vibrational mode because it enables the description of the temperature effect, as well.

Before specializing to a given model, we can explicitly describe the Fourier transform involved in Eq. (2.16). If, as usual, the dipole moments have no diagonal matrix elements, the third-order polarization takes the form

$$\mathbf{P}^{(3)}(\omega)=\frac{i}{\hbar}\sum_{nps}\frac{\boldsymbol{\mu}_{pn}}{i(\omega_{np}-\omega)+\Gamma_{np}}\sum_{\lambda_j j}\int_{-\infty}^{\infty}d\Omega\, e^{i(\omega-\Omega-\omega_j\lambda_j)\bar{t}_j}\frac{2\gamma_j}{(\omega-\Omega-\omega_j\lambda_j)^2+\gamma_j^2}$$
$$\times[\boldsymbol{\mu}_{ns}\cdot\mathbf{E}_j(\lambda_j)\rho_{sp}^{(2)}(\Omega)-\boldsymbol{\mu}_{sp}\cdot\mathbf{E}_j(\lambda_j)\rho_{ns}^{(2)}(\Omega)]\ . \tag{3.1}$$

Here, $|p\rangle$, $|n\rangle$, and $|s\rangle$ are the eigenstates of the molecular system alone. It can be mentioned that we have contributions from both second-order population and coherence terms. Except particular situations, such as those encountered in molecules having permanent dipole moments [38], the population terms are strongly dominant. At this stage, we must evaluate the second-order term of the density matrix. From relation (2.9) and assuming an initial thermalization of the system, we have

$$\rho^{(2)}(t)=-\frac{1}{\hbar^2}\int_{-\infty}^{t}dt_1\int_{-\infty}^{t_1}dt_2\exp\left[-\frac{i}{\hbar}L_0'(t-t_1)\right]L_V(t_1)\exp\left[-\frac{i}{\hbar}L_0'(t_1-t_2)\right]L_V(t_2)\rho(-\infty)\,, \tag{3.2}$$

where

$$\rho(-\infty)=Z^{-1}\sum_{v}|gv\rangle\langle gv|\exp\left[-\frac{E_{gv}}{kT}\right]\,,\quad Z=\sum_{v}\exp\left[-\frac{E_{gv}}{kT}\right]\,. \tag{3.3}$$

This implies a Boltzmann population of the vibrational states $|v\rangle$ in the ground electronic configuration. If only two electronic configurations are coupled by a dipole moment, we get the explicit expression

$$\begin{aligned}\rho_{ij}^{(2)}(t)=-\frac{1}{\hbar^2}\sum_{vv'v''}\frac{e^{-E_{gv}/kT}}{Z}\int_{-\infty}^{t}dt_1\int_{-\infty}^{t_1}dt_2\Bigg\{&\left[\left\langle\!\!\left\langle ij\left|\exp\left[-\frac{i}{\hbar}L_0'(t-t_1)\right]\right|gv\,gv''\right\rangle\!\!\right\rangle L_V(t_1)_{gv\,gv''gv\,ev'}\right.\\&\left.+\left\langle\!\!\left\langle ij\left|\exp\left[-\frac{i}{\hbar}L_0'(t-t_1)\right]\right|ev''ev'\right\rangle\!\!\right\rangle L_V(t_1)_{ev''ev'gv\,ev'}\right]\\&\times e^{(-i\omega_{gv\,ev'})-\Gamma_{gv\,ev'}(t_1-t_2)}L_V(t_2)gv\,ev'gv\,gv\\&+\left[\left\langle\!\!\left\langle ij\left|\exp\left[-\frac{i}{\hbar}L_0'(t-t_1)\right]\right|ev'ev''\right\rangle\!\!\right\rangle L_V(t_1)_{ev'ev''ev'gv}\right.\\&\left.+\left\langle\!\!\left\langle ij\left|\exp\left[-\frac{i}{\hbar}L_0'(t-t_1)\right]\right|gv''gv\right\rangle\!\!\right\rangle L_V(t_1)_{gv''gv\,ev'gv}\right]\\&\times e^{(-i\omega_{ev'gv}-\Gamma_{ev'gv})(t_1-t_2)}L_V(t_2)_{ev'gv\,gv\,gv}\Bigg\}\,,\end{aligned} \tag{3.4}$$

where, for instance,

$$\omega_{gv\,ev'}=(E_{gv}-E_{ev'})/\hbar \tag{3.5}$$

stands for the transition frequency between the states $|gv\rangle$ and $|ev'\rangle$. Then, the evaluation of $\rho_{ij}^{(2)}(t)$ requires the knowledge of the matrix element in the Liouvillian space $\langle\langle ij|\exp[-(i/\hbar)L_0'(t-t_1)]|kl\rangle\rangle$. As long as the states $|k\rangle$ and $|l\rangle$ are different, its expression is quite simple and takes the form

$$\left\langle\!\!\left\langle ij\left|\exp\left[-\frac{i}{\hbar}L_0't\right]\right|kl\right\rangle\!\!\right\rangle=\delta_{ik}\delta_{jl}\exp[(-i\omega_{kl}-\Gamma_{kl})t]\,. \tag{3.6}$$

However, if states $|k\rangle$ and $|l\rangle$ are identical, because of the transition constants, the evaluation becomes more tedious. A simple way of doing it is by introducing the spectral decomposition of the damping operator. Then, we have

$$\begin{aligned}\left\langle\!\!\left\langle ij\left|\exp\left[-\frac{i}{\hbar}L_0't\right]\right|kk\right\rangle\!\!\right\rangle=\sum_{\alpha}&\langle\langle jj|\alpha\alpha\rangle\rangle\\&\times\exp(-\Gamma_{\alpha\alpha\alpha\alpha}t)\\&\times\langle\langle\alpha\alpha|kk\rangle\rangle\delta_{ij}\,,\end{aligned} \tag{3.7}$$

which reduces to a simple diagonalization of the damping operator in the Liouville space. From the previous observations, we can rewrite the required matrix elements into the form

$$\begin{aligned}\rho_{sp}^{(2)}(t)=-\frac{1}{\hbar^2}\sum_{vv'v''}\frac{e^{-E_{gv}/kT}}{Z}\int_{-\infty}^{t}dt_1\int_{-\infty}^{t_1}dt_2\sum_{\theta=\pm1}\Bigg[\Bigg[&\delta_{vv''}\delta_{sp}\sum_{\beta}\langle\langle ss|\beta\beta\rangle\rangle_{\theta}e^{-\Gamma_{\beta\beta\beta\beta}(t-t_1)}\langle\langle\beta\beta|gvgv\rangle\rangle_{\theta}\\&+(1-\delta_{vv''})(\delta_{s\,gv}\delta_{p\,gv''}\delta_{\theta1}+\delta_{p\,gv}\delta_{s\,gv''}\delta_{\theta-1})e^{(-i\theta\omega_{gv\,gv''}-\Gamma_{gv\,gv''})(t-t_1)}\Bigg]\boldsymbol{\mu}_{ev'gv''}(\theta)\sum_{\nu_k,k}\mathbf{E}_k(\nu_k\theta)e^{-it_1\omega_k\nu_k\theta}L_k(t_1)\end{aligned}$$

$$-\left[\delta_{v'v''}\delta_{sp}\sum_{\beta}\langle\langle ss|\beta\beta|\rangle\rangle_{\theta}e^{-\Gamma_{\beta\beta\beta\beta}(t-t_1)}\langle\langle\beta\beta|ev'ev'\rangle\rangle_{\theta}\right.$$
$$\left.+(1-\delta_{v'v''})(\delta_{s\,ev''}\delta_{p\,ev'}\delta_{\theta 1}+\delta_{p\,ev''}\delta_{s\,ev'}\delta_{\theta-1})e^{(-i\theta\omega_{ev''ev'}-\Gamma_{ev''ev'})(t-t_1)}\right]\boldsymbol{\mu}_{ev''gv}(\theta)\sum_{\nu_k,k}\mathbf{E}_k(\nu_k\theta)e^{-it_1\omega_k\nu_k\theta}L_k(t_1)\Bigg]$$
$$\times e^{(-i\theta\omega_{gv\,ev'}-\Gamma_{gv\,ev'})(t_1-t_2)}\boldsymbol{\mu}_{gv\,ev'}(\theta)\sum_{\mu_l,l}\mathbf{E}_l(\mu_l\theta)e^{-it_2\omega_l\mu_l\theta}L_l(t_2)\ . \tag{3.8}$$

Of course, $\rho_{ns}^{(2)}(t)$ can be obtained straightforwardly from the preceding expression by the simple substitution $s\rightarrow n$ and $p\rightarrow s$. For the sake of simplicity, the following notations have been used:

$$\theta=1\Longrightarrow\langle\langle ii|\alpha\alpha\rangle\rangle_{\theta}=\langle\langle ii|\alpha\alpha\rangle\rangle\ ,\quad \boldsymbol{\mu}_{ij}(\theta)=\boldsymbol{\mu}_{ij}\ ,$$
$$\theta=-1\Longrightarrow\langle\langle ii|\alpha\alpha\rangle\rangle_{\theta}=\langle\langle ii|\alpha\alpha\rangle\rangle^{*}\ ,\quad \boldsymbol{\mu}_{ij}(\theta)=\boldsymbol{\mu}_{ji}\ . \tag{3.9}$$

In addition, the matrix elements of the Liouvillian $L_V(t)$, given by

$$L_V(t)_{mnpq}=(-\boldsymbol{\mu}_{mp}\delta_{nq}+\boldsymbol{\mu}_{qn}\delta_{mp})\cdot\sum_{\epsilon_j j}\mathbf{E}_j(\epsilon_j)e^{-it\omega_j\epsilon_j}L_j(t)\ , \tag{3.10}$$

have been introduced. Here, $\Gamma_{ij}$ is the usual dephasing constant defined by

$$\Gamma_{ij}=\tfrac{1}{2}(\Gamma_{ii\,ii}+\Gamma_{jj\,jj})+\Gamma_{ij}^{(d)}\ , \tag{3.11}$$

if $\Gamma_{ij}^{(d)}$ is the pure dephasing constant, $i$ or $j$ standing for either $(gv')$ or $(ev'')$. In the following, it will be convenient to focus on a specific model to make the calculation simpler. This is done in the next section.

## IV. APPLICATION TO A FOUR-LEVEL SYSTEM

At this point, we must specify the molecular system. The simplest model mathematically tractable for our purpose is a four-level model. It implies that at most one vibrational quantum is present in the system. Such a model is depicted in Fig. 1 where the various relaxation and dephasing constants have been introduced.

Now, if the double time integration is performed, we obtain the second-order term $\rho_{sp}^{(2)}(t)$. Its expression can be greatly simplified by introducing again some notations. We first define the functions

$$I(t,A_{\alpha}^{ij})=\exp(A_{\alpha}^{ij}t)/A_{\alpha}^{ij}\ ,$$
$$J(t_1,t_2,A_{\alpha}^{ij})=[\exp(A_{\alpha}^{ij}t_1)-\exp(A_{\alpha}^{ij}t_2)]/A_{\alpha}^{ij}\ , \tag{4.1}$$
$$\overline{H}(t-\tau)=1-H(\tau-t)\ .$$

Also, from the integration over $t_2$, we have

$$W_1(l,B_{\alpha}^{ij})=e^{-\gamma_l\bar{t}_l}I(\bar{t}_l,B_{\alpha}^{ij}+\gamma_l)-e^{\gamma_l\bar{t}_l}I(\bar{t}_l,B_{\alpha}^{ij}-\gamma_l)\ ,$$
$$W_2(l,B_{\alpha}^{ij})=e^{\gamma_l\bar{t}_l}/(B_{\alpha}^{ij}-\gamma_l)\ ,$$
$$W_3(l,B_{\alpha}^{ij})=e^{-\gamma_l\bar{t}_l}/(B_{\alpha}^{ij}+\gamma_l)\ , \tag{4.2}$$
$$a_{1\alpha}^{ij}=0,\quad a_{2\alpha}^{ij}=(B_{\alpha}^{ij}-\gamma_l)\ .$$

From the formal expression given in Appendix A, and taking advantage of the previous notations, we finally get the expression

$$\rho_{sp}^{(2)}(t)=-\frac{1}{\hbar^2}\sum_{vv'v''}\frac{e^{-E_{gv}/kT}}{Z}\sum_{\theta=\pm 1}\sum_{\alpha=1}^{6}\sum_{\nu_k,k}\sum_{\mu_l,l}P_{\alpha}^{sp}e^{C_{\alpha}^{sp}t}$$
$$\times\left[\sum_{n=1}^{2}W_n(l,B_{\alpha}^{sp})\{e^{-\gamma_k\bar{t}_k}[H(t-\bar{t}_k)H(\bar{t}_k-\bar{t}_l)J(\bar{t}_k,\bar{t}_l,A_{\alpha}^{sp}+\gamma_k+a_{n\alpha}^{sp})\right.$$
$$+H(t-\bar{t}_l)\overline{H}(\bar{t}_k-t)H(\bar{t}_k-\bar{t}_l)J(t,\bar{t}_l,A_{\alpha}^{sp}+\gamma_k+a_{n\alpha}^{sp})]$$
$$+e^{\gamma_k\bar{t}_k}[H(t-\bar{t}_k)H(\bar{t}_k-\bar{t}_l)J(t,\bar{t}_k,A_{\alpha}^{sp}-\gamma_k+a_{n\alpha}^{sp})$$
$$+H(t-\bar{t}_l)\overline{H}(\bar{t}_l-\bar{t}_k)J(t,\bar{t}_l,A_{\alpha}^{sp}-\gamma_k+a_{n\alpha}^{sp})]\}$$
$$+W_3(l,B_{\alpha}^{sp})\{e^{-\gamma_k\bar{t}_k}[H(t-\bar{t}_l)H(\bar{t}_k-\bar{t}_l)I(\bar{t}_l,A_{\alpha}^{sp}+B_{\alpha}^{sp}+\gamma_k+\gamma_l)$$
$$+\overline{H}(\bar{t}_l-t)H(\bar{t}_k-\bar{t}_l)I(t,A_{\alpha}^{sp}+B_{\alpha}^{sp}+\gamma_k+\gamma_l)$$
$$+H(t-\bar{t}_k)\overline{H}(\bar{t}_l-\bar{t}_k)I(\bar{t}_k,A_{\alpha}^{sp}+B_{\alpha}^{sp}+\gamma_k+\gamma_l)$$
$$+\overline{H}(\bar{t}_k-t)\overline{H}(\bar{t}_l-\bar{t}_k)I(t,A_{\alpha}^{sp}+B_{\alpha}^{sp}+\gamma_k+\gamma_l)]$$
$$+e^{\gamma_k\bar{t}_k}[H(t-\bar{t}_l)\overline{H}(\bar{t}_l-\bar{t}_k)J(\bar{t}_l,\bar{t}_k,A_{\alpha}^{sp}+B_{\alpha}^{sp}-\gamma_k+\gamma_l)$$
$$\left.+\overline{H}(\bar{t}_l-t)H(t-\bar{t}_k)\overline{H}(\bar{t}_l-\bar{t}_k)J(t,\bar{t}_k,A_{\alpha}^{sp}+B_{\alpha}^{sp}-\gamma_k+\gamma_l)]\}\right]\ . \tag{4.3}$$

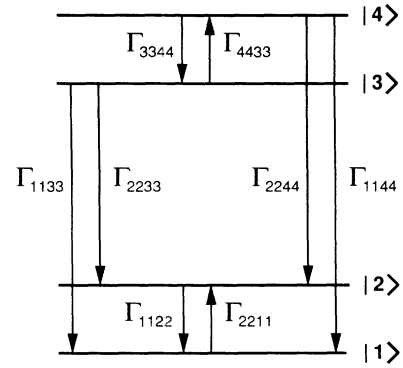

FIG. 1. Energy scheme of the four-level system and the corresponding transition rates of interest in this study.

All the quantities introduced in the preceding expression are defined below. We first describe the symbols corresponding to the population terms. We have for the particular value $\alpha=1$

$$\begin{aligned}P_1^{sp}&=P_1^{sp}(\beta_1)=\delta_{v'v''}\boldsymbol{\mu}_{ev'gv}(\theta)\cdot\mathbf{E}_k(\nu_k\theta)\boldsymbol{\mu}_{gv\,ev'}(\theta)\cdot\mathbf{E}_l(\mu_l\theta)\\&\quad\times(\langle\langle ss|\beta_1\beta_1\rangle\rangle_\theta\langle\langle\beta_1\beta_1|gv\,gv\rangle\rangle_\theta\\&\quad-\langle\langle ss|\beta_1\beta_1\rangle\rangle_\theta\langle\langle\beta_1\beta_1|ev'ev'\rangle\rangle_\theta)\ ,\\A_1^{sp}&=A_1^{sp}(\beta_1)=\Gamma_{\beta_1\beta_1\beta_1\beta_1}-i\theta\omega_k\nu_k-i\theta\omega_{gv\,ev'}-\Gamma_{gv\,ev'}\ ,\\B_1^{sp}&=B_1^{sp}(\beta_1)=-i\theta\omega_l\mu_l+i\theta\omega_{gv\,ev'}+\Gamma_{gv\,ev'}\ ,\end{aligned}\tag{4.4}$$

and next for $\alpha=2,3,4$

$$\begin{aligned}P_\alpha^{sp}&=P_1^{sp}(\beta_\alpha)\ ,\\A_\alpha^{sp}&=A_1^{sp}(\beta_\alpha)\ ,\\B_\alpha^{sp}&=B_1^{sp}(\beta_\alpha)\ .\end{aligned}\tag{4.5}$$

Finally, we give the symbols introduced in the coherence terms. We just have

$$\begin{aligned}P_5^{sp}&=P_5^{sp}(\beta_5)=(1-\delta_{v\,v''})(\delta_{s\,gv}\delta_{p\,gv''}\delta_{\theta 1}+\delta_{p\,gv}\delta_{s\,gv''}\delta_{\theta-1})\\&\quad\times\boldsymbol{\mu}_{ev'gv''}(\theta)\cdot\mathbf{E}_k(\nu_k\theta)\boldsymbol{\mu}_{gv\,ev'}(\theta)\cdot\mathbf{E}_l(\mu_l\theta)\ ,\\P_6^{sp}&=P_6^{sp}(\beta_6)=-(1-\delta_{v'v''})(\delta_{s\,ev''}\delta_{p\,ev'}\delta_{\theta 1}+\delta_{p\,ev''}\delta_{s\,ev'}\delta_{\theta-1})\\&\quad\times\boldsymbol{\mu}_{ev''gv}(\theta)\cdot\mathbf{E}_k(\nu_k\theta)\boldsymbol{\mu}_{gv\,ev'}(\theta)\cdot\mathbf{E}_l(\mu_l\theta)\ ,\\A_5^{sp}&=A_5^{sp}(\beta_5)=-i\theta\omega_k\nu_k+i\theta\omega_{gv\,gv''}+\Gamma_{gv\,gv''}\\&\quad-i\theta\omega_{gv\,ev'}-\Gamma_{gv\,ev'}\ ,\\A_6^{sp}&=A_6^{sp}(\beta_6)=-i\theta\omega_k\nu_k+i\theta\omega_{ev''ev'}+\Gamma_{ev''ev'}\\&\quad-i\theta\omega_{gv\,ev'}-\Gamma_{gv\,ev'}\ ,\\B_5^{sp}&=B_5^{sp}(\beta_5)+B_1^{sp}\\B_6^{sp}&=B_6^{sp}(\beta_5)=B_1^{sp}\ .\end{aligned}\tag{4.6}$$

The second contributions $\rho_{ns}^{(2)}(t)$ are obtained similarly. Because the transient hole-burning spectra have been expressed in terms of the Fourier transform of the polarization, we still require the Fourier transform of $\rho^{(2)}(t)$ established to calculate $\mathbf{P}^{(3)}(\omega)$ given by Eq. (3.1). Taking advantage of the formal result given in Appendix B and introducing the notation

$$\begin{aligned}C_\alpha^{sp}&=-\Gamma_{\beta_\alpha\beta_\alpha\beta_\alpha\beta_\alpha},\quad \alpha=1,2,3,4\ ,\\C_5^{sp}&=-i\theta\omega_{gv\,gv''}-\Gamma_{gv\,gv''}\ ,\\C_6^{sp}&=-i\theta\omega_{ev''ev'}-\Gamma_{ev''ev'}\ ,\end{aligned}\tag{4.7}$$

we obtain $\rho_{sp}^{(2)}(\Omega)$ in the form

$$\begin{aligned}\rho_{sp}^{(2)}(\Omega)=-\frac{1}{\hbar^2}\sum_{vv'v''}\frac{e^{-E_{gv}/kT}}{Z}&\sum_{\theta=\pm1}\sum_{\alpha=1}^{6}\sum_{\nu_k,k}\sum_{\mu_l,l}P_\alpha^{sp}\\\times\Bigg\{\sum_{n=1}^{2}W_n(l,B_\alpha^{sp})&\Bigg[-e^{-\gamma_k\bar{t}_k}H(\bar{t}_k-\bar{t}_l)\frac{J(\bar{t}_k,\bar{t}_l,i\Omega+C_\alpha^{sp}+A_\alpha^{sp}+\gamma_k+a_{n\alpha}^{sp})}{i\Omega+C_\alpha^{sp}}\\&+e^{\gamma_k\bar{t}_k}H(\bar{t}_k-\bar{t}_l)\frac{I(\bar{t}_k,i\Omega+C_\alpha^{sp}+A_\alpha^{sp}-\gamma_k+a_{n\alpha}^{sp})}{i\Omega+C_\alpha^{sp}}+e^{\gamma_k\bar{t}_k}\overline{H}(\bar{t}_l-\bar{t}_k)\frac{I(\bar{t}_l,i\Omega+C_\alpha^{sp}+A_\alpha^{sp}-\gamma_k+a_{n\alpha}^{sp})}{i\Omega+C_\alpha^{sp}}\Bigg]\\+W_3(l,B_\alpha^{sp})&\Bigg[e^{\gamma_k\bar{t}_k}\overline{H}(\bar{t}_l-\bar{t}_k)\frac{J(\bar{t}_k,\bar{t}_l,i\Omega+C_\alpha^{sp}+A_\alpha^{sp}+B_\alpha^{sp}-\gamma_k+\gamma_l)}{i\Omega+C_\alpha^{sp}}\\&-e^{-\gamma_k\bar{t}_k}H(\bar{t}_k-\bar{t}_l)\frac{I(\bar{t}_l,i\Omega+C_\alpha^{sp}+A_\alpha^{sp}+B_\alpha^{sp}+\gamma_k+\gamma_l)}{i\Omega+C_\alpha^{sp}}\\&-e^{-\gamma_k\bar{t}_k}\overline{H}(\bar{t}_l-\bar{t}_k)\frac{I(\bar{t}_k,i\Omega+C_\alpha^{sp}+A_\alpha^{sp}+B_\alpha^{sp}+\gamma_k+\gamma_l)}{i\Omega+C_\alpha^{sp}}\Bigg]\Bigg\}\ .\end{aligned}\tag{4.8}$$

By performing the last integration, we get the frequency-dependent third-order polarization which is required for the evaluation of the transient hole-burning spectrum. It can be written as

$$\begin{aligned}\mathbf{P}^{(3)}(\omega)=&-\frac{i}{\hbar^3}\sum_{n,p,s}\frac{\boldsymbol{\mu}_{pn}}{i(\omega_{np}-\omega)+\Gamma_{np}}\sum_{\lambda_j,j}\sum_{v_k,k}\sum_{\mu_l,l}\sum_{v,v',v''}\frac{e^{-E_{gv}/kT}}{Z}\sum_{\theta=\pm 1}\sum_{\alpha}\Bigg| P_\alpha^{sp}\boldsymbol{\mu}_{ns}\cdot\mathbf{E}_j(\lambda_j)\\ &\times\Bigg\{\sum_{m=1}^{2}W_m(l,B_\alpha^{sp})\{e^{-\gamma_k\bar{t}_k}H(\bar{t}_k-\bar{t}_l)[F(W_1,\bar{t}_l)-F(W_1,\bar{t}_k)]+e^{\gamma_k\bar{t}_k}[H(\bar{t}_k-\bar{t}_l)F(W_2,\bar{t}_k)+\bar{H}(\bar{t}_l-\bar{t}_k)F(W_2,\bar{t}_l)]\}\\ &+W_3(l,B_\alpha^{sp})\{e^{\gamma_k\bar{t}_k}\bar{H}(\bar{t}_l-\bar{t}_k)[F(W_4,\bar{t}_k)-F(W_4,\bar{t}_l)]-e^{-\gamma_k\bar{t}_k}[H(\bar{t}_k-\bar{t}_l)F(W_3,\bar{t}_l)+\bar{H}(\bar{t}_l-\bar{t}_k)F(W_3,\bar{t}_k)]\}\Bigg\}\\ &-P_\alpha^{ns}\boldsymbol{\mu}_{sp}\cdot\mathbf{E}_j(\lambda_j)\left\{\sum_{m=1}^{2}W_m(l,B_\alpha^{ns})\{sp\to ns\}+W_3(l,B_\alpha^{ns})\{sp\to ns\}\right\}\Bigg| \ . \end{aligned} \tag{4.9}$$

The terms in the curly brackets of the preceding expression $\{sp\to ns\}$ correspond to the ones above except that now the quantities are evaluated by simple substitution from the matrix element $\rho_{sp}^{(2)}(t)$. For the sake of convenience, the following parameters have been introduced:

$$\begin{aligned} &W_0=i\Omega+C_\alpha^{sp} \ ,\\ &W_1=A_\alpha^{sp}+\gamma_k+a_{n\alpha}^{sp} \ ,\\ &W_2=A_\alpha^{sp}-\gamma_k+a_{n\alpha}^{sp} \ ,\\ &W_3=A_\alpha^{sp}+B_\alpha^{sp}+\gamma_k+\gamma_l \ ,\\ &W_4=A_\alpha^{sp}+B_\alpha^{sp}-\gamma_k+\gamma_l \ . \end{aligned} \tag{4.10}$$

Also the functions $F(W_i,\bar{t})$ have been defined from the convolution product. They take the form

$$\begin{aligned} F(W_i,\bar{t})=&\int_{-\infty}^{\infty}d\Omega\, e^{i(\omega-\Omega-\omega_j\lambda_j)\bar{t}_j}\frac{2\gamma_j}{(\omega-\Omega-\omega_j\lambda_j)^2+\gamma_j^2}\frac{e^{(W_0+W_i)\bar{t}}}{W_0(W_0+W_i)}\\ =&\Bigg[\frac{2\pi e^{\gamma_j\bar{t}_j}}{C_\alpha^{sp}-\gamma_j+i(\omega-\omega_j\lambda_j)}I(\bar{t},W_i+C_\alpha^{sp}-\gamma_j+i(\omega-\omega_j\lambda_j))\\ &+\frac{4\pi\gamma_j e^{\gamma_j\bar{t}_j}}{W_i[W_i+C_\alpha^{sp}+\gamma_j+i(\omega-\omega_j\lambda_j)]}I(\bar{t}_j,W_i+C_\alpha^{sp}-\gamma_j+i(\omega-\omega_j\lambda_j))\bar{H}(\mathrm{Re}(W_i+C_\alpha^{sp}))\Bigg]H(\bar{t}-\bar{t}_j)\\ &-\Bigg[\frac{-2\pi e^{-\gamma_j\bar{t}_j}}{C_\alpha^{sp}+\gamma_j+i(\omega-\omega_j\lambda_j)}I(\bar{t},W_i+C_\alpha^{sp}+\gamma_j+i(\omega-\omega_j\lambda_j))\\ &+\frac{4\pi\gamma_j e^{-\gamma_j\bar{t}_j}}{W_i[W_i+C_\alpha^{sp}-\gamma_j+i(\omega-\omega_j\lambda_j)]}I(\bar{t}_j,W_i+C_\alpha^{sp}+\gamma_j+i(\omega-\omega_j\lambda_j))\bar{H}(-\mathrm{Re}(W_i+C_\alpha^{sp}))\\ &-\frac{4\pi\gamma_j e^{-\gamma_j\bar{t}_j}}{[C_\alpha^{sp}-\gamma_j+i(\omega-\omega_j\lambda_j)]}I(\bar{t}_j,C_\alpha^{sp}+\gamma_j+i(\omega-\omega_j\lambda_j))I(\bar{t},W_i)\Bigg]\bar{H}(\bar{t}_j-\bar{t}) \ . \end{aligned} \tag{4.11}$$

Therefore we have established all the expressions which are required to evaluate the transient hole-burning spectrum. In the next section, we will select the contributions participating in the third-order polarization for a given geometry of the experiment. Also, to simplify the results, we will introduce the rotating-wave approximation.

## V. TRANSIENT HOLE-BURNING SPECTRUM

The transient hole-burning spectrum is obtained from the attenuation of the probe beam as a function of the frequency. Therefore the phase-matched terms giving the main contributions to the spectrum correspond to some particular combinations. These terms will be generated by the $\mathbf{k}_p$ component of the polarization. They can be obtained by selecting the appropriate terms in the previous expression (4.9), involving two interactions with the pump beam and only one with the probe beam. Therefore just three terms contribute, and they correspond to the chronological ordering

$$l=e,\quad k=e,\quad j=p \Longrightarrow E_p(t_1)E_e(t_2)E_e(t_3)\ , \tag{5.1a}$$

$$l=e,\quad k=p,\quad j=e \Longrightarrow E_e(t_1)E_p(t_2)E_e(t_3)\ , \tag{5.1b}$$

$$l=e,\quad k=p,\quad j=e \Longrightarrow E_e(t_1)E_e(t_2)E_p(t_3)\ , \tag{5.1c}$$

if $t_1 \geq t_2 \geq t_3$. The resonant terms, which survive when the rotating-wave approximation (RWA) is introduced into the second-order population, are given by the values $\mu_l=-1$ and $\nu_k=1$. Next, in the expression of the third-order polarization, the resonant terms in the $\mathbf{k}_p$ direction are obtained by taking the appropriate values of $\lambda_j$ and $\theta$. The first resonant contribution denoted (5.1a) just above characterizes, in a diagrammatical scheme, the pathways and their complex conjugates required to build up the second-order population and the subsequent third-order polarization. They correspond to the values $\lambda=1$, $\theta=\pm 1$. Next, the second resonant contribution (5.1b) is obtained for the values $\lambda=1$, $\theta=+1$, because the $\mathbf{k}_e$ component does not contribute. Similarly, the last resonant contribution (5.1c) corresponds to $\lambda=1$, $\theta=-1$.

Finally, to get a complete analytical expression of the transient hole-burning spectrum, we still require an explicit development of the spectral decomposition introduced for the free evolution of the system. Here, because of the transition rate constants, the Liouvillian representation of the free evolution is not diagonal in the zero-order basis. A simple diagonalization gives the eigenvalues:

$$\begin{aligned}
\Gamma_{\beta_1\beta_1\beta_1\beta_1} &= 0\ ,\\
\Gamma_{\beta_2\beta_2\beta_2\beta_2} &= \Gamma_{1111}+\Gamma_{2222}\ ,\\
\Gamma_{\beta_3\beta_3\beta_3\beta_3} &= \tfrac{1}{2}\{(\Gamma_{3333}+\Gamma_{4444})\\
&\qquad -[(\Gamma_{3333}-\Gamma_{4444})^2+4\Gamma_{3344}\Gamma_{4433})]^{1/2}\}\ ,\\
\Gamma_{\beta_4\beta_4\beta_4\beta_4} &= \tfrac{1}{2}\{(\Gamma_{3333}+\Gamma_{4444})\\
&\qquad +[(\Gamma_{3333}-\Gamma_{4444})^2+4\Gamma_{3344}\Gamma_{4433})]^{1/2}\}\ .
\end{aligned} \tag{5.2}$$

Next, we must evaluate the overlappings. In fact, we just need the product of the overlappings. They can be obtained directly from the Laplace transform of the equations for the free evolution. The results are listed below for $i \neq j$:

$$\begin{aligned}
\langle\langle pp|\beta_i\beta_i\rangle\rangle\langle\langle\beta_i\beta_i|pp\rangle\rangle &= \frac{-\Gamma_{\beta_i\beta_i\beta_i\beta_i}+\Gamma_{(p+1)(p+1)(p+1)(p+1)}}{\Gamma_{\beta_j\beta_j\beta_j\beta_j}-\Gamma_{\beta_i\beta_i\beta_i\beta_i}}\ ,\quad p=1;\ i,j=1,2 \ \text{ or }\ p=3;\ i,j=3,4\ ,\\
\langle\langle pp|\beta_i\beta_i\rangle\rangle\langle\langle\beta_i\beta_i|pp\rangle\rangle &= \frac{-\Gamma_{\beta_i\beta_i\beta_i\beta_i}+\Gamma_{(p-1)(p-1)(p-1)(p-1)}}{\Gamma_{\beta_j\beta_j\beta_j\beta_j}-\Gamma_{\beta_i\beta_i\beta_i\beta_i}},\quad p=2;\ i,j=1,2 \ \text{ or }\ p=4;\ i,j=3,4\ ,\\
\langle\langle pp|\beta_i\beta_i\rangle\rangle\langle\langle\beta_i\beta_i|(p+1)(p+1)\rangle\rangle &= \frac{-\Gamma_{pp(p+1)(p+1)}}{\Gamma_{\beta_j\beta_j\beta_j\beta_j}-\Gamma_{\beta_i\beta_i\beta_i\beta_i}},\quad p=1;\ i,j=1,2 \ \text{ or }\ p=3;\ i,j=3,4\ ,\\
\langle\langle pp|\beta_i\beta_i\rangle\rangle\langle\langle\beta_i\beta_i|(p-1)(p-1)\rangle\rangle &= \frac{-\Gamma_{pp(p-1)(p-1)}}{\Gamma_{\beta_j\beta_j\beta_j\beta_j}-\Gamma_{\beta_i\beta_i\beta_i\beta_i}},\quad p=2;\ i,j=1,2 \ \text{ or }\ p=4;\ i,j=3,4\ ,\\
\langle\langle nn|\beta_i\beta_i\rangle\rangle\langle\langle\beta_i\beta_i|mm\rangle\rangle &= -1\Big/\prod_{j\neq i=1}^{4}(\Gamma_{\beta_j\beta_j\beta_j\beta_j}-\Gamma_{\beta_i\beta_i\beta_i\beta_i})\\
&\quad\times\left[\begin{pmatrix} -\Gamma_{\beta_i\beta_i\beta_i\beta_i}+\Gamma_{2222} & -\Gamma_{1122}\\ -\Gamma_{2211} & -\Gamma_{\beta_i\beta_i\beta_i\beta_i}+\Gamma_{1111}\end{pmatrix}\begin{pmatrix}\Gamma_{1133} & \Gamma_{1144}\\ \Gamma_{2233} & \Gamma_{2244}\end{pmatrix}\right.\\
&\quad\left.\times\begin{pmatrix} -\Gamma_{\beta_i\beta_i\beta_i\beta_i}+\Gamma_{4444} & -\Gamma_{3344}\\ -\Gamma_{4433} & -\Gamma_{\beta_i\beta_i\beta_i\beta_i}+\Gamma_{3333}\end{pmatrix}\right]_{n(m-2)}\ ,\\
&\qquad i=1,4 \ \text{ for }\ n=1,2 \ \text{ and }\ m=3,4\ .
\end{aligned} \tag{5.3}$$

Therefore we have now established the expression of the transient hole-burning spectrum for the four-level system. It will be useful, in the next sections, to discuss the influence of the artifact contributions, as well as to analyze the role of the dephasing processes and temperature effects, in such an experiment.

## VI. INFLUENCE OF FIELDS AND DYNAMICS ON THE DIFFERENTIAL TRANSMITTANCE

From the expression of the transient hole-burning spectrum or its corresponding differential transmittance $\Delta\alpha(\omega)$ previously established, we introduce some numerical calculations to emphasize the influence of the physical parameters, such as the spectral linewidth of the laser beams, the time delay of the pulses, and the relaxation and dephasing constants of the molecular system.

To start this discussion, we first consider the variations of the differential transmittance with the time delay between the pump and the probe pulses $\tau_{pe}$. This calculation has been done for two different ranges of pump spectral widths associated typically to femtosecond and picosecond time scales. They correspond to Figs. 2 and 3,

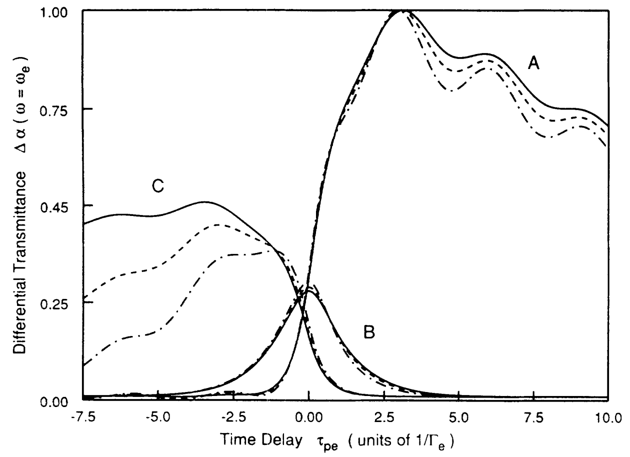

FIG. 2. Differential transmittance in arbitrary units plotted as a function of the time delay $\tau_{pe}$. The ground and excited vibrational frequencies are both 100 $\text{cm}^{-1}$, and $\omega=\omega_p=\omega_e=\omega_{31}=\omega_{42}=15\,000\ \text{cm}^{-1}$. Curves *A*, *B*, and *C* are the level population, pump polarization coupling, and perturbed free-induction-decay terms, for different values of the pure dephasing. Solid, short-dashed, and dot-dashed lines correspond to $\Gamma_{13}^{(d)}=\Gamma_{24}^{(d)}=0$, 5, and 15 $\text{cm}^{-1}$, respectively. The other parameters are $\Gamma_{12}^{(d)}=\Gamma_{14}^{(d)}=\Gamma_{23}^{(d)}=\Gamma_{34}^{(d)}=0$, $\Gamma_{1122}=\Gamma_{3344}=-15\ \text{cm}^{-1}$, $\Gamma_{1133}=\Gamma_{1144}=\Gamma_{2233}=\Gamma_{2244}=-1\ \text{cm}^{-1}$, $\mu_{13}=\mu_{24}=0.6$, $\mu_{23}=\mu_{14}=0.3$, $T=0$ K, $\Gamma_p=500\ \text{cm}^{-1}$, and $\Gamma_e=50\ \text{cm}^{-1}$.

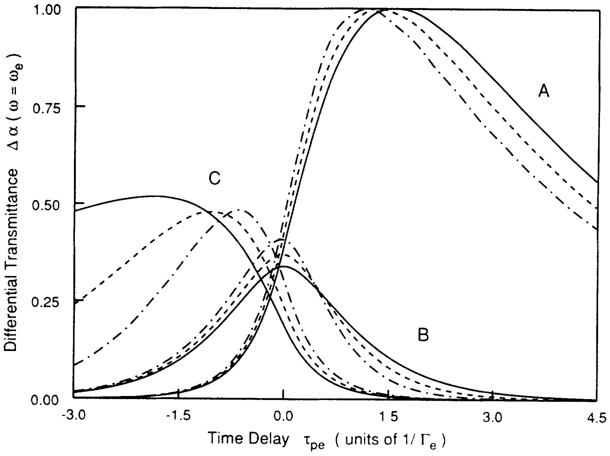

FIG. 3. Differential transmittance in arbitrary units corresponding to the same parameters as in Fig. 2 except $\Gamma_p=500\ \text{cm}^{-1}$ and $\Gamma_e=10\ \text{cm}^{-1}$.

respectively. The pump and the probe beams are degenerate and resonant with the electronic transition, so that $\omega_p=\omega_e=\omega_{31}$. For the frequency $\omega=\omega_{31}$, we represent, at zero temperature, the three components of the differential transmittance $\Delta\alpha(\omega_{31})$. The main component, labeled *A*, comes from the traditional hole-burning term where the population is burned as a consequence of two interactions between the pump beam and the molecular system, and is next tested by a spectrally broader probe beam. This contribution increases with the time duration of the probe and decays subsequently with the lifetime of the excited state $|3\rangle$. When the spectral width of the pump pulse is not large enough to induce a coherent excitation of the vibrational levels, the decay of the differential transmittance is monotonic, as shown in Fig. 3. These contributions *A* have been termed $S_0$ and $S_1$ level populations, as they result from the populations created by the pump in the ground $S_0$ and excited $S_1$ electronic configurations. In the opposite case sketched in Fig. 2 and attainable in some femtosecond experiments, we observe an oscillatory decay of frequency $\omega=\omega_{21}=\omega_{43}$ if the vibrational frequencies are degenerate, or more complex oscillations if the vibrational frequencies are different. This variation results from two contributions. The first one is due to the populations created by the pump pulse in the $S_0$ and $S_1$ electronic configurations, and the second one arises from coherences induced between the vibrational levels of the same electronic configuration. The overall decrease of the differential transmittance follows the time constant $T_1$ of the level 3. However, the oscillatory structure, whose frequency characterizes the vibrational pattern of the molecular system, is damped with the dephasing time $T_2$ of the corresponding vibrational levels [39]. These quantum beat effects are well known, and have been described and observed experimentally in the literature [40–45]. In their works on impulsive stimulated Raman scattering [44,45], Chesnoy and Mokhtari have observed that vibrational excitation occurs in the ground and in the excited configuration as well. The changes of the probe pulse amplitude depend on the excited electronic configuration, while dispersion effects, inducing a phase perturbation of the probe, arise from the ground electronic states. With their experimental setup, they performed the measurements of the vibrational oscillatory decay of malachite green, with different types of solvents, by measuring the dephasing time from induced birefringence and frequency modulation experiments in the ground electronic state, and induced absorption and amplitude modulation experiments for the excited electronic configuration. Next the contribution labeled *B* results from the chronological ordering pump-probe-pump of the interactions. It requires the simultaneous interactions of the molecule with the pump and the probe pulses, and increases with the overlap of the pulses. This contribution, termed the $S_0$ and $S_1$ pump polarization coupling term, is generated by the diffraction of the pump by the grating created previously by the pump-and-probe pulses. Its time extension at half maximum is of the order of $2/\Gamma_e$. The last contribution, designated by *C*, is dominant when the probe pulse precedes the pump pulse. It is termed the $S_0$ and $S_1$ perturbed free-induction-decay term. It increases with a time constant of the order of the dephasing times and exhibits oscillations which are specific for the differences between electronic transitions and field frequency. Finally, the increase of the pure dephasing $\Gamma_{13}^{(d)}=\Gamma_{24}^{(d)}$, by acting on the dephasing time $T_2$, decreases the overall response of the three contributions. It does not affect their time delay dependence [39], except for the perturbed free-induction-decay term, as can be seen in various previous works [16,20,24,26].

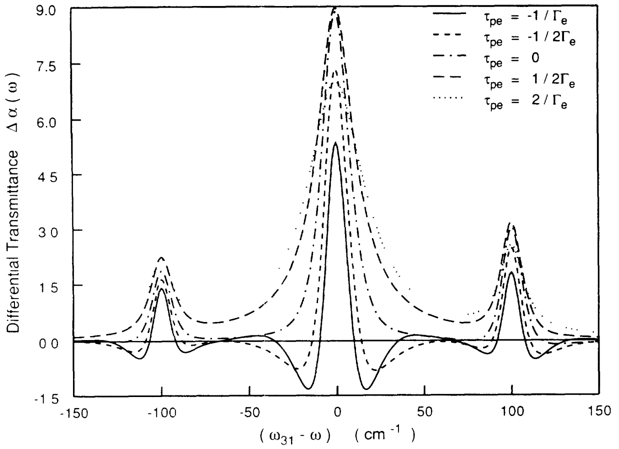

FIG. 4. The differential transmittance is calculated in arbitrary units for different delay times $\tau_{pe}$ as a function of the frequency detuning $(\omega-\omega_{31})$. The other parameters are the same as in Fig. 3, and $\Gamma_{13}^{(d)}=\Gamma_{24}^{(d)}=20\ \text{cm}^{-1}$.

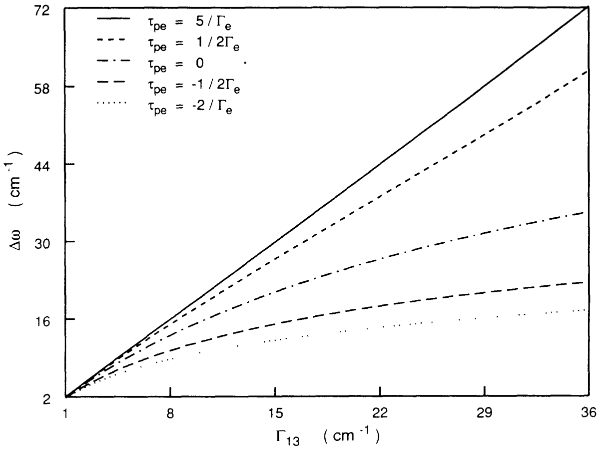

FIG. 5. Numerical FWHM of the central line shape as a function of the dephasing between levels 1 and 3, with $\Gamma_{13}^{(d)}=\Gamma_{24}^{(d)}$, for different time delay $\tau_{pe}$. Other parameters are the same as in Fig. 2, except $\Gamma_p=900\ \text{cm}^{-1}$ and $\Gamma_e=25\ \text{cm}^{-1}$.

Next, we consider the frequency dependence of the differential transmittance. Figure 4 exhibits these variations for various time delays $\tau_{pe}$. The two sidebands are corresponding to the transition frequencies $\omega_{32}$ and $\omega_{41}$ and the main peak accounts for the pure electronic transition frequencies $\omega_{31}$ and $\omega_{42}$, as it has been observed in dynamic hole-burning experiments on cresyl violet [20]. Again, we consider a zero temperature and the pump frequency resonant with the electronic transition. For the sake of simplicity, we assume a spectral width of the pump pulse narrow enough to avoid a coherent excitation of the vibrational levels, as stated in most of the hole-burning experiments. When the time delay is smaller than $-1/\Gamma_e$, the main contribution comes from the perturbed free-induction-decay term. If $\tau_{pe}$ increases, the pump polarization coupling term starts contributing too. For coincident pulses, i.e., $\tau_{pe}=0$, all the contributions are of the same importance. Then, for positive values of $\tau_{pe}$, the usual hole-burning term corresponding to the $S_0$ and $S_1$ level population term is predominant. The artifacts have negligible contribution and the linewidth of the main peak becomes proportional to the value of the dephasing between levels 1 and 3, say $\Delta\alpha=2\Gamma_{13}$. If we focus on this particular case, as shown in Fig. 5, it is not possible to relate in a simple way the linewidth of the central peak to the various parameters of the molecule and fields if either the two pulses overlap or the probe pulse precedes the pump pulse. The total contribution decreases with a time constant corresponding to the lifetime of the excited electronic state. This well-known result has been observed on transient absorption spectra of typical organic dyes in various solvents [47], as well as in low-temperature glasses of resorufin in glycerol, ethanol, and *d*-ethanol [48].

## VII. TEMPERATURE EFFECTS IN TRANSIENT HOLE BURNING

This last section is dedicated to the study of the temperature dependence on the hole-burning spectrum. To this end, from expression (3.1) corresponding to the Fourier transform of the third-order polarization, and restricting the description to the central peak of Fig. 4, that is to say, to light fields resonant with the pure electronic transition $\omega_{31}$ or $\omega_{42}$, we obtain

$$\begin{aligned}\mathbf{P}^{(3)}(\omega)\simeq\frac{i}{\hbar}\sum_{\lambda_j,j}\int_{-\infty}^{\infty}d\Omega\, e^{i(\omega-\Omega-\omega_j\lambda_j)\bar{t}_j}\frac{2\gamma_j}{(\omega-\Omega-\omega_j\lambda_j)^2+\gamma_j^2}\\ \times\mathbf{E}_j(\lambda_j)\cdot\left\{\frac{1}{i(\omega_{31}-\omega)+\Gamma_{31}}[\boldsymbol{\mu}_{31}\rho_{11}^{(2)}(\Omega)-\boldsymbol{\mu}_{41}\rho_{34}^{(2)}(\Omega)-\boldsymbol{\mu}_{31}\rho_{33}^{(2)}(\Omega)+\boldsymbol{\mu}_{32}\rho_{21}^{(2)}(\Omega)]\boldsymbol{\mu}_{13}\right.\\ \left.+\frac{1}{i(\omega_{42}-\omega)+\Gamma_{42}}[\boldsymbol{\mu}_{41}\rho_{12}^{(2)}(\Omega)-\boldsymbol{\mu}_{42}\rho_{44}^{(2)}(\Omega)-\boldsymbol{\mu}_{32}\rho_{43}^{(2)}(\Omega)+\boldsymbol{\mu}_{42}\rho_{22}^{(2)}(\Omega)]\boldsymbol{\mu}_{24}\right\}.\end{aligned}\tag{7.1}$$

For large time delay, such that $\tau_{pe}\gg 1/\Gamma_e$, the dominant contribution to the polarization comes from the hole-burning term. In addition, we assume a spectrally narrow pump beam so that the second-order coherence in Eq. (7.1) can be neglected. Because in the usual transient hole-burning experiment, the spectral distribution $\gamma_p$ of the probe beam is very large with respect to $\gamma_e$ and to any spectral characteristic of the molecules, we can approximate the convolution product by

$$
\begin{aligned}
\mathbf{P}^{(3)}(\omega) \simeq {} & \frac{i}{\hbar}\frac{2}{\gamma_p}\frac{\boldsymbol{\mu}_{13}}{i(\omega_{31}-\omega)+\Gamma_{31}}\boldsymbol{\mu}_{31}\cdot\mathbf{E}_p(1) \\
& \times\int_{-\infty}^{\infty} d\Omega[\rho_{11}^{(2)}(\Omega)-\rho_{33}^{(2)}(\Omega)] \\
& +\frac{i}{\hbar}\frac{2}{\gamma_p}\frac{\boldsymbol{\mu}_{24}}{i(\omega_{42}-\omega)+\Gamma_{42}}\boldsymbol{\mu}_{42}\cdot\mathbf{E}_p(1) \\
& \times\int_{-\infty}^{\infty} d\Omega[\rho_{22}^{(2)}(\Omega)-\rho_{44}^{(2)}(\Omega)] \ . 
\end{aligned} \tag{7.2}
$$

With $\omega_{21}=\omega_{43}=U$, we can approximate the second-order population terms for levels 2 and 4, which can be written as

$$
\begin{aligned}
\rho_{22}^{(2)}(\Omega) &\simeq e^{-U/kT}\rho_{11}^{(2)}(\Omega) \ , \\
\rho_{44}^{(2)}(\Omega) &\simeq e^{-U/kT}\rho_{33}^{(2)}(\Omega) \ ,
\end{aligned} \tag{7.3}
$$

since for large time delay, the thermal equilibrium is established between the vibrational levels. Also, with an initial thermalized population and a pump beam well-defined energetically, so that only transitions 1-3 or 2-4 are resonant, the population of the ground electronic configuration is just transferred to the excited one. If we assume

$$
\begin{aligned}
&\boldsymbol{\mu}=\boldsymbol{\mu}_{24}=\boldsymbol{\mu}_{13} \ , \\
&\omega_{31}-\omega=\omega_{42}-\omega=W-\omega \ ,
\end{aligned} \tag{7.4}
$$

and parallel polarizations of the fields, we obtain the third-order polarization in the form

$$
\begin{aligned}
\mathbf{P}^{(3)}(\omega) \simeq {} & \frac{i}{\hbar}\frac{2}{\gamma_p}\boldsymbol{\mu}\cdot\mathbf{E}_p(1)\boldsymbol{\mu} \\
& \times\left[\frac{1}{i(W-\omega)+\Gamma_{31}}+\frac{e^{-U/kT}}{i(W-\omega)+\Gamma_{42}}\right] \\
& \times\int_{-\infty}^{\infty} d\Omega[\rho_{11}^{(2)}(\Omega)-\rho_{33}^{(2)}(\Omega)] \ .
\end{aligned} \tag{7.5}
$$

From the definition of the differential transmittance given by the relation (1.1) and neglecting the frequency dependence of $\mathbf{E}_p(\omega)$ and $\omega$ over the frequency range of interest, we obtain

$$
\Delta\alpha(\omega)\simeq\frac{\Gamma_{31}}{(W-\omega)^2+\Gamma_{31}^2}+e^{-U/kT}\frac{\Gamma_{42}}{(W-\omega)^2+\Gamma_{42}^2} \ . \tag{7.6}
$$

With the notation

$$
\Gamma_{42}^{*}=\Gamma_{42}+e^{-U/kT}\Gamma_{31} \tag{7.7}
$$

the full width at half maximum (FWHM) is expressed by

$$
\begin{aligned}
\Delta\omega=\sqrt{2}\Bigg[ & -(\Gamma_{31}^2-\Gamma_{42}^2)\left[1-2\frac{\Gamma_{42}}{\Gamma_{42}^{*}}\right] \\
& +\left\{\left[(\Gamma_{31}^2-\Gamma_{42}^2)\left[1-2\frac{\Gamma_{42}}{\Gamma_{42}^{*}}\right]\right]^2 \right. \\
& \left. +4\Gamma_{31}^2\Gamma_{42}^2\right\}^{1/2}\Bigg]^{1/2} \ .
\end{aligned} \tag{7.8}
$$

At $T=0$, the well-known result

$$
\begin{aligned}
&\Delta\omega=2\Gamma_{31} \ , \\
&\Delta\alpha(\omega)\simeq\frac{\Gamma_{31}}{(W-\omega)^2+\Gamma_{31}^2}
\end{aligned} \tag{7.9}
$$

is recovered. When the temperature increases, the temperature-dependent term in Eq. (7.6) alters the original behavior described by a single Lorentzian. We have now a sum of two Lorentzian curves, the second one being weighted by a Boltzmann factor. This is true as long as the inhomogeneous broadening can be neglected. The simple linear law between the FWHM and the electronic dephasing is no longer valid in experiments which are performed at room temperatures.

It has to be noted that, if the pure electronic dephasing is independent of the temperature and such that $\Gamma_{31}^{(d)}=\Gamma_{42}^{(d)}$, only the dephasing constant $\Gamma_{31}$ is temperature dependent through the relaxation constants of levels 1 and 3. Then, if the conditions

$$
\begin{aligned}
&e^{-U/kT}\ll 1 \ , \\
&\Gamma_{31}\ll\Gamma_{42}
\end{aligned} \tag{7.10}
$$

are satisfied, we have

$$
\Delta\omega=2\Gamma_{31}\left[1+\frac{\Gamma_{31}}{\Gamma_{42}}e^{-U/kT}\right] \ , \tag{7.11}
$$

and we recover the linear dependence of $\Delta\omega$ with $\Gamma_{31}$ at low temperature, as used in the experiments performed on glasses. In these works, temperature behavior of the electronic dephasing is taken into account by power laws [49–51], or by a mixing between power laws and Arrhenius temperature dependence [48].

In Fig. 6, we show the temperature dependence of $\Delta\omega$, either from the simple model discussed previously and giving the dependence of Eq. (7.6) or by extracting numerically $\Delta\omega$ from the exact calculation (7.1) established in the preceding section. This comparison has been done

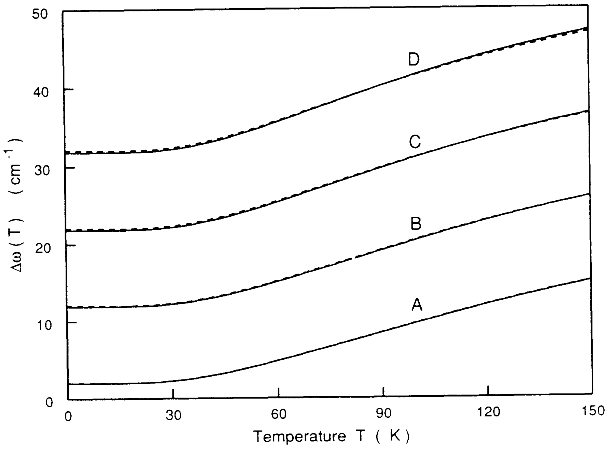

FIG. 6. Temperature dependence of FWHM plotted for different values of the pure dephasing. Numerical and analytical results are shown as solid and dashed lines, respectively. Curves *A*, *B*, *C*, and *D* correspond to $\Gamma_{13}^{(d)}=\Gamma_{24}^{(d)}=0$, 5, 10, and 15 cm$^{-1}$. The other parameters are given in Fig. 2, except $\Gamma_p=900$ cm$^{-1}$, $\Gamma_e=30$ cm$^{-1}$. $\tau_{pe}\approx 15/\Gamma_e$.

for different values of the pure dephasing. We observe a good agreement between these two evaluations, which validates our approximation.

Next, we compare the variations of $\Delta\omega$, given by Eq. (7.6), with respect to the limiting value $\Delta\omega_0=2\Gamma_{31}$ as a function of the temperature. This is done in Fig. 7 for different values of the pure dephasing. For temperature of the order of 30 K or lower, the agreement between the exact results and the two-resonance model previously introduced is quite good. In addition, for a given temperature, as the pure dephasing becomes more important, we observe an increasing deviation of $\Delta\omega$ with respect to $2\Gamma_{31}$, due to the growing contribution of $\Gamma_{42}$ in $\Delta\omega$.

Finally, in Fig. 8, we show the variation of the ratio $\Delta\omega/2\Gamma_{31}$. It has been seen in the previous figure that the pure dephasing increases the difference $\Delta\omega-2\Gamma_{31}$. In fact, this variation is not monotonic, as it could be thought from Fig. 7. To clarify this point, we increase $\Gamma^{d}_{31}$, chosen here equal to $\Gamma^{(d)}_{42}$, up to the limiting value $\Gamma_{31}/\Gamma_{42}\approx 1$. The dotted curves represent the variations of $\Delta\omega/2\Gamma_{31}$ obtained from Eq. (7.8). Also we note that the curves corresponding to different temperatures start at different values of the ratio $\Gamma_{31}/\Gamma_{42}$. This is due to the fact that the minimum value of $\Gamma_{31}/\Gamma_{42}$ is temperature dependent. For increasing values of the ratio, we observe that the full line corresponding to the exact evaluation of $\Delta\omega(T)$ differs notably from $\Delta\omega/2\Gamma_{31}$ given by Eq. (7.8). This discrepancy is due to the overlapping of the resonances at $\omega=\omega_{41}$ and $\omega_{32}$ with the one at $\omega=\omega_{31}$ and $\omega_{42}$, when the broadening of the central peak is increased. Then, $\Delta\omega/2\Gamma_{31}$ reaches a maximum which varies with the temperature and next decreases toward 1. This is because, when the pure dephasing increases, we have $\Gamma_{31}\simeq\Gamma_{42}\simeq\Gamma$ and Eq. (7.6) becomes

$$\Delta\alpha(\omega)\simeq(1+e^{-U/kT})\frac{\Gamma}{(W-\omega)^2+\Gamma^2} \tag{7.12}$$

so that we recover the behavior of a two-level system characterized by a single Lorentzian with a linewidth $\Delta\omega\simeq 2\Gamma$, instead of the four-level system previously considered.

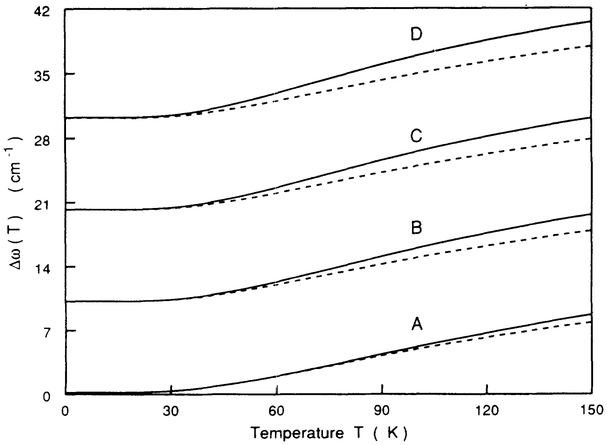

FIG. 7. The temperature dependence of the FWHM is represented by the solid lines for the values of the pure dephasing chosen in Fig. 5. Dashed lines correspond to $\Delta\omega(T)=2\Gamma_{13}$, for $\Gamma_{1122}=\Gamma_{1144}=-10$ cm$^{-1}$. Other parameters are defined in Fig. 6.

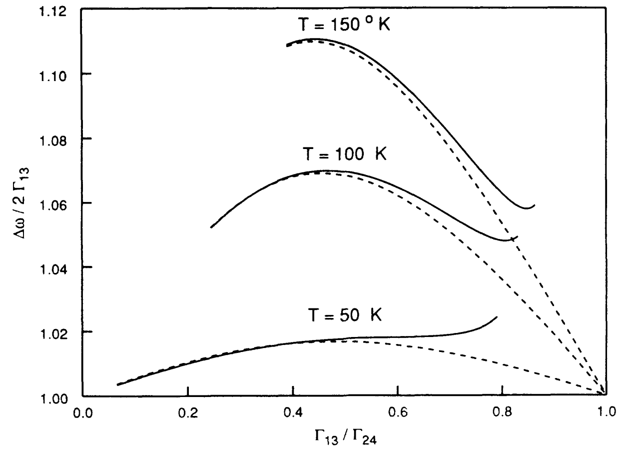

FIG. 8. The ratio of FWHM over $2\Gamma_{13}$ is plotted vs the ratio $\Gamma_{13}/\Gamma_{24}$, for increasing values of the pure dephasing $\Gamma^{(d)}_{13}=\Gamma^{(d)}_{24}$. Numerical and analytical results correspond to solid and dashed lines, respectively. The case of different values of the temperature has been considered. The other parameters are the same as in Fig. 7.

## VIII. CONCLUSION

In this work, we have reported a theoretical treatment of ultrafast transient hole-burning experiments. In this approach, valid when the pump and the probe pulses overlap, the hole burning is described as a completely general four-wave-mixing process. From this description, the various contributions participating in the hole burning have been shown for systems undergoing relaxation and pure dephasing processes, as well. From their comparison, it has been possible to stress the importance of the coherent artifact as a function of the time delay between the pulses. In addition, the influence of the dephasing processes on these contributions has been emphasized. Next, the frequency dependence of the differential transmittance has been analyzed for the same internal parameters, previously discussed. Finally, the influence of the temperature on the differential transmittance has been studied. Although the general expression has been established analytically, a simple model has been deduced which gives a very good agreement with the exact result, at least for low temperature in a physical situation where the usual hole-burning term is dominant.

## ACKNOWLEDGMENTS

Arizona State University Center for the Study of Early Events in Photosynthesis is funded by the U.S. Department of Energy (U.S. DOE) Grant No. DE-FG02-88ER 1969 as part of the U.S. Department of Agriculture–U.S. DOE–National Science Foundation Plant Science Center Program. This work was supported in part by NATO.

## APPENDIX A

The formal time integral required for the double-sided exponential envelope is given here. The quantities $W_n(l,B_\alpha)$ and $a_{n\alpha}$ are defined in the text. For simplicity, the upper indices have been omitted.

$$\begin{aligned}
&\int_{-\infty}^{t} dt_1 \int_{-\infty}^{t_1} dt_2 e^{A_\alpha t_1} e^{B_\alpha t_2} [e^{\gamma_k (t_1-\bar{t}_k)} \overline{H}(\bar{t}_k - t_1) + e^{-\gamma_k (t_1-\bar{t}_k)} H(t_1-\bar{t}_k)][e^{\gamma_l (t_2-\bar{t}_l)} \overline{H}(\bar{t}_l - t_2) + e^{-\gamma_l (t_2-\bar{t}_l)} H(t_2-\bar{t}_l)] \\
&\quad = \sum_{n=1}^{2} W_n(l,B_\alpha) \{ e^{-\gamma_k \bar{t}_k} [H(t-\bar{t}_k) H(\bar{t}_k-\bar{t}_l) J(\bar{t}_k, \bar{t}_l, A_\alpha + \gamma_k + a_{n\alpha}) \\
&\qquad\qquad\qquad + H(t-\bar{t}_l) \overline{H}(\bar{t}_k - t) H(\bar{t}_k - \bar{t}_l) J(t, \bar{t}_l, A_\alpha + \gamma_k + a_{n\alpha})] \\
&\qquad\qquad + e^{\gamma_k \bar{t}_k} [H(t-\bar{t}_k) H(\bar{t}_k - \bar{t}_l) J(t, \bar{t}_k, A_\alpha - \gamma_k + a_{n\alpha}) \\
&\qquad\qquad\qquad + H(t-\bar{t}_l) \overline{H}(\bar{t}_l - \bar{t}_k) J(t, \bar{t}_l, A_\alpha - \gamma_k + a_{n\alpha})]\} \\
&\qquad + W_3(l,B_\alpha) \{ e^{-\gamma_k \bar{t}_k} [H(t-\bar{t}_l) H(\bar{t}_k - \bar{t}_l) I(\bar{t}_l, A_\alpha + B_\alpha + \gamma_k + \gamma_l) \\
&\qquad\qquad\qquad + \overline{H}(\bar{t}_l - t) H(\bar{t}_k - \bar{t}_l) I(t, A_\alpha + B_\alpha + \gamma_k + \gamma_l) \\
&\qquad\qquad\qquad + H(t-\bar{t}_k) \overline{H}(\bar{t}_l - \bar{t}_k) I(\bar{t}_k, A_\alpha + B_\alpha + \gamma_k + \gamma_l) \\
&\qquad\qquad\qquad + \overline{H}(\bar{t}_k - t) \overline{H}(\bar{t}_l - \bar{t}_k) I(t, A_\alpha + B_\alpha + \gamma_k + \gamma_l)] \\
&\qquad\qquad + e^{\gamma_k \bar{t}_k} [H(t-\bar{t}_l) \overline{H}(\bar{t}_{l\,-}\bar{t}_k) J(\bar{t}_l, \bar{t}_k, A_\alpha + B_\alpha - \gamma_k + \gamma_l) \\
&\qquad\qquad\qquad + \overline{H}(\bar{t}_l - t) H(t-\bar{t}_k) \overline{H}(\bar{t}_l - \bar{t}_k) J(t, \bar{t}_k, A_\alpha + B_\alpha - \gamma_k + \gamma_l)]\} \;. 
\end{aligned} \tag{A1}$$

## APPENDIX B

We give here the formal result of the Fourier transform of the time-dependent term presented in Appendix A:

$$\begin{aligned}
&\int_{-\infty}^{+\infty} dt\, e^{(C_\alpha + i\Omega)t} \int_{-\infty}^{t} dt_1 \int_{-\infty}^{t_1} dt_2 e^{A_\alpha t_1} e^{B_\alpha t_2} [e^{\gamma_k (t_1-\bar{t}_k)} \overline{H}(\bar{t}_k - t_1) + e^{-\gamma_k (t_1-\bar{t}_k)} H(t_1-\bar{t}_k)] \\
&\qquad\qquad\qquad \times [e^{\gamma_l (t_2-\bar{t}_l)} \overline{H}(\bar{t}_l - t_2) + e^{-\gamma_l (t_2-\bar{t}_l)} H(t_2-\bar{t}_l)] \\
&\quad = \sum_{n=1}^{2} W_n(l,B_\alpha) \Bigg[ -e^{-\gamma_k \bar{t}_k} H(\bar{t}_k - \bar{t}_l) \frac{J(\bar{t}_k, \bar{t}_l, i\Omega + C_\alpha + A_\alpha + \gamma_k + a_{n\alpha})}{i\Omega + C_\alpha} \\
&\qquad\qquad + e^{\gamma_k \bar{t}_k} H(\bar{t}_k - \bar{t}_l) \frac{I(\bar{t}_k, i\Omega + C_\alpha + A_\alpha - \gamma_k + a_{n\alpha})}{i\Omega + C_\alpha} \\
&\qquad\qquad + e^{\gamma_k \bar{t}_k} \overline{H}(\bar{t}_l - \bar{t}_k) \frac{I(\bar{t}_l, i\Omega + C_\alpha + A_\alpha - \gamma_k + a_{n\alpha})}{i\Omega + C_\alpha} \Bigg] \\
&\qquad + W_3(l,B_\alpha) \Bigg[ e^{\gamma_k \bar{t}_k} \overline{H}(\bar{t}_l - \bar{t}_k) \frac{J(\bar{t}_k, \bar{t}_l, i\Omega + C_\alpha + A_\alpha + B_\alpha - \gamma_k + \gamma_l)}{i\Omega + C_\alpha} \\
&\qquad\qquad - e^{-\gamma_k \bar{t}_k} H(\bar{t}_k - \bar{t}_l) \frac{I(\bar{t}_l, i\Omega + C_\alpha + A_\alpha + B_\alpha + \gamma_k + \gamma_l)}{i\Omega + C_\alpha} \\
&\qquad\qquad - e^{-\gamma_k \bar{t}_k} \overline{H}(\bar{t}_l - \bar{t}_k) \frac{I(\bar{t}_k, i\Omega + C_\alpha + A_\alpha + B_\alpha + \gamma_k + \gamma_l)}{i\Omega + C_\alpha} \Bigg] \;.
\end{aligned} \tag{B1}$$

---

[1] B. M. Kharlamov, R. I. Personov, and L. A. Bykovkaya, Opt. Commun. **12**, 191 (1974).

[2] H. de Vries and D. A. Wiersma, Phys. Rev. Lett. **36**, 91 (1976).

[3] S. Völker, R. M. Macfarlane, A. Z. Genack, H. P. Trommsdorff, and J. H. van der Waals, J. Chem. Phys. **67**, 1759 (1977).

[4] Y. S. Bai and M. D. Fayer, Chem. Phys. **128**, 135 (1988).

[5] W. B. Bosma, Y. J. Yan, and S. Mukamel, J. Chem. Phys. **93**, 3863 (1990).

[6] J. R. Andrews, R. M. Hochstrasser, and H. P. Trommsdorff, Chem. Phys. **62**, 87 (1981).

[7] N. Morita and T. Yajima, Phys. Rev. A **30**, 2525 (1984).

[8] J. J. Song, J. H. Lee, and M. D. Levenson, Phys. Rev. A **17**, 1439 (1978).

[9] Y. S. Bai and M. D. Fayer, Phys. Rev. B **39**, 11 066 (1989).

[10] S. Völker, Annu. Rev. Phys. Chem. **40**, 499 (1989).

[11] C. R. Giuliano and L. D. Hess, Appl. Phys. Lett. **9**, 196 (1966).

[12] M. L. Spaeth and W. R. Sooy, J. Chem. Phys. **48**, 2315

(1968).

[13] G. Mourou, IEEE J. Quantum Electron. **QE-11**, 1 (1975).

[14] R. Menzel and P. Witte, J. Chem. Phys. **87**, 6769 (1987).

[15] R. A. Mathies, C. H. Brito Cruz, W. T. Pollard, and C. V. Shank, Science **240**, 777 (1988).

[16] W. T. Pollard, C. H. Brito Cruz, C. V. Shank, and R. A. Mathies, J. Chem. Phys. **90**, 199 (1989).

[17] S. H. Lin, B. Fain, and N. Hamer, Adv. Chem. Phys. **79**, 133 (1990).

[18] S. Mukamel, Annu. Rev. Phys. Chem. **41**, 647 (1990).

[19] S. H. Lin, R. G. Alden, R. Islampour, H. Ma, and A. A. Villaeys, *Density Matrix Methods and Femtosecond Processes* (World Scientific, Singapore, 1991).

[20] C. H. Brito Cruz, R. L. Fork, W. H. Knox, and C. V. Shank, Chem. Phys. Lett. **132**, 341 (1986).

[21] A. M. Weiner, S. De Silvestri, and E. Ippen, J. Opt. Soc. Am. B **2**, 654 (1985).

[22] C. V. Shank, P. C. Becker, H. L. Fragnito, and R. L. Fork, in *Ultrafast Phenomena,* edited by T. Yajima, K. Yoshihara, C. B. Harris, and S. Shionoya (Springer, New York, 1988), Vol. 6, p. 344.

[23] E. T. J. Nibbering, D. Wiersma, and K. Duppen, Phys. Rev. Lett. **66**, 2464 (1991).

[24] C. H. Brito Cruz, J. P. Gordon, P. C. Becker, R. L. Fork, and C. V. Shank, IEEE J. Quantum Electron. **QE-24**, 261 (1988).

[25] H. A. Ferwerda, J. Terpstra, and D. A. Wiersma, J. Chem. Phys. **91**, 3296 (1989).

[26] T. J. Kang, J. Yu, and M. Berg, J. Chem. Phys. **94**, 2413 (1991).

[27] T. J. Kang, J. Yu, and M. Berg, Chem. Phys. Lett. **174**, 476 (1990).

[28] S. R. Meech, A. J. Hoff, and D. A. Wiersma, Chem. Phys. Lett. **121**, 287 (1985).

[29] S. G. Boxer, D. J. Lockhart, and T. R. Middendorf, Chem. Phys. Lett. **123**, 476 (1986).

[30] J. K. Gillie, B. L. Fearey, J. M. Hayes, G. J. Small, and J. H. Golbeck, Chem. Phys. Lett. **134**, 316 (1987).

[31] J. K. Gillie, B. L. Fearey, J. M. Hayes, G. J. Small, and J. H. Golbeck, J. Phys. Chem. **92**, 4012 (1988).

[32] J. Friedrich, J. D. Swalen, and D. Haarer, J. Chem. Phys. **73**, 705 (1980).

[33] L. Kador, D. Haarer, and R. Personov, J. Chem. Phys. **86**, 5300 (1987).

[34] R. F. Loring, Y. J. Yan, and S. Mukamel, J. Chem. Phys. **87**, 5840 (1987).

[35] H. Graener, T. Lösch, and A. Laubereau, J. Chem. Phys. **93**, 5365 (1990).

[36] H. Graener and A. Laubereau, J. Phys. Chem. **95**, 3447 (1991).

[37] M. D. Levenson and S. S. Kano, *Introduction to Nonlinear Laser Spectroscopy* (Academic, New York, 1988), Sec. 2.9.

[38] J. P. Lavoine, C. Hoerner, and A. A. Villaeys, Phys. Rev. A **44**, 5947 (1991).

[39] G. Stock, and W. Domcke, Phys. Rev. A **45**, 3032 (1992).

[40] M. Mitsunaga and C. L. Tang, Phys. Rev. A **35**, 1720 (1987).

[41] I. A. Wamsley, M. Mitsunaga, and C. L. Tang, Phys. Rev. A **38**, 4681 (1988).

[42] M. J. Rosker, F. W. Wise, and C. L. Tang, Phys. Rev. Lett. **57**, 321 (1986).

[43] F. W. Wise, M. J. Rosker, and C. L. Tang, J. Chem. Phys. **86**, 2827 (1987).

[44] A. Mokhtari and J. Chesnoy, Europhys. Lett. **5**, 523 (1988).

[45] J. Chesnoy and A. Mokhtari, Phys. Rev. A **38**, 3566 (1988).

[46] J. Yu, T. J. Kang, and M. Berg, J. Chem. Phys. **94**, 5787 (1991).

[47] S. Kinoshita, H. Itoh, H. Murakami, H. Miyasaka, T. Okada, and N. Mataga, Chem. Phys. Lett. **166**, 123 (1990).

[48] M. Berg, C. A. Walsh, L. R. Narasimhan, K. A. Littau, and M. D. Fayer, J. Chem. Phys. **88**, 1564 (1988).

[49] A. I. M. Dicker, L. W. Johnson, S. Völker, and J. H. van der Waals, Chem. Phys. Lett. **100**, 8 (1983).

[50] P. J. van der Zaag, B. C. Schokker, T. Schmidt, R. M. Macfarlane, and S. Völker, J. Lumin. **45**, 80 (1990).

[51] P. J. van der Zaag, J. P. Galaup, and S. Völker, Chem. Phys. Lett. **166**, 263 (1990).